HHS Public Access

Author manuscript

Endoscopy. Author manuscript; available in PMC 2019 August 01.

Published in final edited form as:

Endoscopy. 2019 April ; 51(4): 355–359. doi:10.1055/a-0725-7995.

Assessment of Barrett's esophagus and dysplasia with ultrahigh-speed volumetric en face and cross-sectional optical coherence tomography

Osman O. Ahsen[1], **Kaicheng Liang**[1], **Hsiang-Chieh Lee**[1], **Michael G. Giacomelli**[1], **Zhao Wang**[1], **Benjamin Potsaid**[1,2], **Marisa Figueiredo**[3], **Qin Huang**[3,4], **Vijaysekhar Jayaraman**[5], **James G. Fujimoto**[1], **Hiroshi Mashimo**[3,4]

[1]Department of Electrical Engineering and Computer Science and Research Laboratory of Electronics, Massachusetts Institute of Technology, Cambridge, Massachusetts, United States

[2]Thorlabs, Inc., Newton, NewJersey, United States

[3]VA Boston Healthcare System, Boston, Massachusetts, United States

[4]Harvard Medical School, Boston, Massachusetts, United States

[5]Praevium Research, Inc., Santa Barbara, California, United States

Abstract

Background—This study aimed to evaluate the use of ultra-high-speed volumetric en face and cross-sectional optical coherence tomography (OCT) with micromotor catheters for the in vivo assessment of Barrett's esophagus and dysplasia.

Methods—74 OCT datasets with correlated biopsy/endoscopic mucosal resection histology (49 nondysplastic Barrett's esophagus [NDBE], 25 neoplasia) were obtained from 14 patients with Barrett's esophagus and a history of dysplasia and 30 with NDBE. The associations between irregular mucosal patterns on en face OCT, absence of mucosal layering, surface signal>subsurface, and>5 atypical glands on cross-sectional OCT vs. histology and treatment history were assessed by three blinded readers.

Results—Atypical glands under irregular mucosal patterns occurred in 75% of neoplasia (96% of treatment-naÏve neoplasia) vs. 30% of NDBE datasets (43% of short- and 18% of long-segment NDBE). Mucosal layering was absent in 35% of neoplasia and 50% of NDBE datasets, and surface signal >subsurface occurred in 29% of neoplasia and 30% of NDBE datasets.

Conclusions—Atypical glands under irregular mucosal patterns are strongly associated with neoplasia, suggesting potential markers for dysplasia and a role in pathogenesis.

Corresponding author Hiroshi Mashimo, MD, PhD, Gastroenterology Section, VA Boston Healthcare System, Harvard Medical School, Boston, MA, 02130, United States Fax: +1-857-203-5666 hmashimo@hms.harvard.edu.

Competing interests

None

Introduction

Barrett's esophagus surveillance is limited by biopsy sampling error. Narrow-band imaging (NBI) [1] and confocal laser endomicroscopy [2] can improve sensitivity for identifying dysplasia. Optical coherence tomography (OCT) [3] enables microscopic resolution and high-speed volumetric imaging and is commercially available as volumetric laser endomicroscopy (VLE; Nine-Point Medical, Bedford, Massachusetts, USA) [4]. Studies have investigated cross-sectional OCT dysplasia features [5], including a diagnostic algorithm (VLE-DA) [6]; however, many previous VLE studies used ex vivo specimens because of challenges in registering biopsy with OCT. We previously demonstrated ultrahigh-speed endoscopic OCT that was > 10-times faster than commercial instruments, enabling depth-resolved en face and cross-sectional imaging [7]. The aim of the current study was to investigate volumetric en face and cross-sectional OCT for identifying neoplasia.

Methods

Study setting and data acquisition

Imaging was conducted at VA Boston Healthcare System (VABHS) under an institutional review board-approved protocol at VABHS, Harvard Medical School, and Massachusetts Institute of Technology. Patients with Barrett's esophagus (14with a history of dysplasia and 30 with nondysplastic Barrett's esophagus [NDBE]) who were undergoing endoscopic surveillance or therapy were imaged between September 2013 and March 2017.

Dual-channel endoscopes enabled direct visualization of OCT catheter positioning and subsequent biopsy/endoscopic mucosal resection (EMR) from the OCT-imaged region; however, biopsy/EMR was not guided in real time (►Fig.e1; supplementary material is available online). Ultrahigh-speed OCT, at 600 000 A-scans/second with micromotor catheters, scanned a ~ 10mmxl6mmarea (Appendix e1, ►Fig.e2, ►Table e1) at the 6 o'clock position from the gastroesophageal junction to the squamocolumnar junction and also regions with nodularity and/or irregular mucosal/vascular patterns on white-light endoscopy (WLE)/NBI.

OCT datasets were categorized as NDBE if correlated histology indicated NDBE, and as neoplasia if histology indicated low grade dysplasia (LGD), high grade dysplasia (HGD) or esophageal adenocarcinoma (EAC). NDBE datasets from patients with a history of dysplasia were not used because features may differ from the normal NDBE population. An experienced gastrointestinal pathologist (Q.H.) made the histology diagnosis, with confirmation from expert referral centers (Appendix e2, ►Table e2).

Reading criteria and methodology

An investigator (O.O.A.) who did not participate in the study readings developed the reading criteria. Depth-resolved en face OCT criteria were regular vs. irregular mucosal patterns [1] (►Fig. 3)> and cross-sectional OCT criteria were absence of mucosal layering, surface signal >subsurface, and >5 atypical glands, similarly to published VLE-DA features [6] (Appendix e3, ►Fig.e4).

Three readers with differing endoscopy/OCT experience who were blinded to the histological diagnoses read the OCT datasets. A total of 13 datasets were used for training and 7 datasets were used for pretest (Appendix e4, ►Table e3). Blinded readings were performed on 54 datasets (37 NDBE, 6 LGD, 9 HGD, 2 EAC). Readers assessed depth-resolved en face OCT, followed by cross-sectional OCT (►Fig.5, Appendix e4). Readers recorded the position and depth of en face features and image location of cross-sectional features, as well as confidence (“high”/“low”), and reading times. Statistical methods are described in Appendix e5.

Results

Patient and dataset characteristics

A total of 74 OCT datasets with correlated biopsy/EMR histology were obtained (►Table e4; 49 NDBE, 10 LGD, 13 HGD, 2 EAC). A total of 12/25 (48%) neoplasia datasets were from treatment-naÏve patients (n = 10) and 13/25 (52%) were from previously treated patients (ablation/EMR, n = 8), four of whom were also imaged when treatment naÏve.

Reading results

Readers’ pooled assessments are reported. For en face OCT, readers identified irregular mucosal patterns in 100% of neoplasia datasets vs. 35% of NDBE datasets (P<0.001) with 43% in short- and 28% in long-segment NDBE (►Table e5). For cross-sectional OCT, mucosal layering was absent in 35% of neoplasia datasets (21 % in the treatment-naÏve subgroup) and 50% of NDBE datasets. Surface signal>subsurface occurred in 29% of neoplasia datasets (21 % in the treatment-naÏve subgroup) and 30% of NDBE datasets (►Table e6). Atypical glands (>5) were present in 75% of neoplasia (96% in the treatmentnaÏve subgroup) and 59% of NDBE datasets (►Table e5). These numbers represent the independent occurrences of features anywhere within the datasets.

The co-location of en face and cross-sectional features was also evaluated. Atypical glands were present (co-localized) under irregular mucosal patterns in 75% of neoplasia vs. 30% of NDBE datasets (►Table 7; *P*<0.001). Atypical glands under irregular mucosal patterns were present in 96% of treatmentnaÏve neoplasia, 43% of short-segment NDBE, and only 18 % of long-segment NDBE. Within the long-segment NDBE subgroup, atypical glands under irregular mucosal patterns were present predominantly near the gastroesophageal junction (25% ≤ 3 cm vs. 14% >3cm from the junction).

Interobserver agreement was substantial (kappa = 0.73) for irregular mucosal patterns, moderate (kappa = 0.6) for absent mucosal layering, poor (kappa = 0.17) for surface signal Subsurface, and substantial (kappa = 0.73) for atypical glands (►Table e8). Average reading times for en face and cross-sectional features were 60±51 seconds and 69 ± 42 seconds, respectively (►Table e9).

Discussion

Early in vivo OCT studies using cross-sectional images reported 70%−80% sensitivity/specificity for dysplasia [8–9]. VLE can image ~ 6cm lengths of esophagus using balloon

catheters, but speeds are insufficient to obtain en face OCT. Leggett et al. developed a VLE-DA showing 86% sensitivity and 88 % specificity with ex vivo specimens from 27 patients [6]. Swager et al. used VLE-DA features with a scoring-based criteria, achieving 83% sensitivity and 71% specificity with ex vivo specimens from 29 patients [5]. These studies had precise registration of OCT with histology; however, feature appearance may differ in vivo.

We used depth-resolved en face OCT to assess mucosal patterns as well as cross-sectional features. Mucosal pattern size/ shape varied among patients (►Fig.3), consistent with NBI observations. We included larger numbers of patients with NDBE in order to achieve adequate representation. Despite the similarity to NBI, en face OCT has different contrast mechanisms and resolution (Appendix e6). OCT can visualize subsurface features, with deeper structures affected by optical attenuation and scattering from superficial structures [10]. ►Table e1 compares ultrahigh-speed endoscopic OCT with other modalities.

En face OCT irregular mucosal patterns were present in 1 00 % of neoplasia datasets; however, there was a selection bias because most datasets were obtained from regions with nodularity and/or irregular mucosal/vascular patterns on WLE/NBI. Irregular mucosal patterns were also present in 35 % of NDBE datasets. Cross-sectional OCT features of absent mucosal layering and surface signal > subsurface were present in 35 % and 29% of neoplasia, but also in 50% and 30% of NDBE datasets. This high rate in NDBE might be caused by biopsy sampling error (Appendix e7), motion artifacts (►Fig.5), distortion from OCT catheter pressure (Appendix e7), or inherently low specificity. Biopsy/EMR was not guided under real-time OCT and our study was not designed to compare OCT with WLE/ NBI. Future studies with laser marking should improve histological correlation [11].

The association of atypical glands and irregular mucosal patterns is a key finding of our study. Atypical glands were present under irregular mucosal patterns in 75% of neoplasia datasets and 96% of treatment-naÏve neoplasia. Conversely, atypical glands under irregular mucosal patterns were present in 30% of NDBE datasets ($P<0.001$ for neoplasia vs. NDBE). Further stratifying by Barrett's esophagus length showed atypical glands under irregular mucosal patterns in 43% of short-segment vs. 18% of long-segment NDBE ($P=0.005$). Within the long-segment NDBE subgroup, atypical glands under irregular mucosal patterns were predominantly present near the gastroesophageal junction (25%≤3cm vs. 14%>3cm from the junction; $P = 0.28$). Cardiac glands occur near the gastroesophageal junction [12] and were not distinguishable from atypical glands, so they may have been misinterpreted as atypical glands (Appendix e7). Atypical glands under irregular mucosal patterns were strongly associated with neoplasia. Furthermore, atypical glands occurred more frequently than irregular mucosal patterns (Appendix e8), which is consistent with the pathogenesis literature, suggesting that atypical glands may be a precursor to irregular mucosal patterns and dysplasia [13].

Atypical glands under irregular mucosal patterns or independently might be a marker for dysplasia, especially in proximal regions of long-segment Barrett's esophagus where interpretation is not confounded by cardiac glands and where dysplasia frequently occurs [14]. Further investigation is needed to determine whether OCT can differentiate between

atypical and cardiac glands. The cross-sectional features of absent mucosal layering and surface signal>subsurface had poor association with neoplasia even in treatment-naÏve cases and were often present in NDBE (►Table e6).

OCT data can be viewed using combined en face and crosssectional OCT “orthoplane” visualization, where readers can rapidly assess the entire volume using depth-resolved en face OCT, identify regions of interest, then assess cross-sectional OCT in these regions before final classification. Orthoplane reading is rapid, reduces burden of assessing thousands of cross-sectional OCT images, and provides information not available in en face or cross-sectional views alone.

The supplement provides additional information on: association of mucosal patterns with cross-sectional features, histological diagnosis and treatment history (Appendix e8, ►Table e10), association of en face OCT and VLE-DA criteria with histological diagnosis and treatment history (Appendix e9, ►Table e11), an LGD subgroup analysis (Appendix e2), and readers’ confidence and reading times (Appendix e10, ►Table e9, ►Table e12).

Study limitations include small sample size, particularly for dysplastic/treatment-naÏve patients. Most patients with neoplasia had undergone ablation/EMR treatment. Although inclusion of previously treated patients is common in OCT/NBI literature [1, 6], some features were associated with treatment history (►Table 7, ►Table e5). Furthermore, reading was performed retrospectively. Prospective studies on larger cohorts of treatment-naÏve and/or general Barrett’s esophagus surveillance patients are needed.

Supplementary Material

Refer to Web version on PubMed Central for supplementary material.

Acknowledgment

This work was supported in part by the VA Boston Healthcare System (facility support), National Institutes of Health grants R01-CA075289 – 20 (J.G.F. and H.M.), R01-CA178636 – 04 and R01-EY011289 – 30 (J.G.F.), Air Force Office of Scientific Research contracts FA9550 – 15 – 1-0473 and FA9550 – 12 – 1-0499 (J.G.F.), Agency for Science, Technology and Research graduate fellowship, Singapore (K.L.).

References

[1]. Sharma P, Bergman JJ, Goda K et al. Development and validation of a classification system to identify high-grade dysplasia and esophageal adenocarcinoma in Barrett’s esophagus using narrowband imaging. Gastroenterology 2016; 150: 591–598 [PubMed: 26627609]

[2]. Canto MI. Endomicroscopy of Barrett’s esophagus. Gastroenterol Clin North Am 2010; 39: 759–769 [PubMed: 21093753]

[3]. Adler DC, Chen Y, Huber R et al. Three-dimensional endomicroscopy using optical coherence tomography. Nature Photonics 2007; 1: 709–716

[4]. Wolfsen HC, Sharma P, Wallace MB et al. Safety and feasibility of volumetric laser endomicroscopy in patients with Barrett’s esophagus (with videos). Gastrointest Endosc 2015; 82: 631–640 [PubMed: 25956472]

[5]. Swager AF, Tearney GJ, Leggett CL et al. Identification of volumetric laser endomicroscopy features predictive for early neoplasia in Barrett’s esophagus using high-quality histological correlation. Gastrointest Endosc 2017; 85: 918–926.e7 [PubMed: 27658906]

[6]. Leggett CL, Gorospe EC, Chan DK et al. Comparative diagnostic performance of volumetric laser endomicroscopy and confocal laser endomicroscopy in the detection of dysplasia associated with Barrett's esophagus. Gastrointest Endosc 2016; 83: 880–888.2 [PubMed: 26344884]

[7]. Tsai TH, Ahsen OO, Lee HC et al. Endoscopic optical coherence angiography enables 3-dimensional visualization of subsurface microvasculature. Gastroenterology 2014; 147: 1219–1221 [PubMed: 25172015]

[8]. Isenberg G, Sivak MV Jr., Chak A et al. Accuracy of endoscopic optical coherence tomography in the detection of dysplasia in Barrett's esophagus: a prospective, double-blinded study. Gastrointest Endosc 2005; 62: 825–831 [PubMed: 16301020]

[9]. Evans JA, Poneros JM, Bouma BE et al. Optical coherence tomography to identify intramucosal carcinoma and high-grade dysplasia in Barrett's esophagus. Clin Gastroenterol Hepatol 2006; 4: 38–43 [PubMed: 16431303]

[10]. Liang K, Ahsen OO, Lee HC et al. Volumetric mapping of Barrett's esophagus and dysplasia with en face optical coherence tomography tethered capsule. Am J Gastroenterol 2016; 111: 1664–1666 [PubMed: 27808130]

[11]. Alshelleh M, Inamdar S, McKinley M et al. Incremental yield of dysplasia detection in Barrett's esophagus using volumetric laser endomicroscopy with and without laser marking compared with a standardized random biopsy protocol. Gastrointest Endosc 2018; 88: 35–42 [PubMed: 29410080]

[12]. Gupta N, Siddiqui U, Waxman I et al. Use of volumetric laser endomicroscopy for dysplasia detection at the gastroesophageal junction and gastric cardia. World J Gastrointest Endosc 2017;9:319–326 [PubMed: 28744344]

[13]. McDonald SA, Lavery D, Wright NA et al. Barrett oesophagus: lessons on its origins from the lesion itself. Nat Rev Gastroenterol Hepatol 2015; 12: 50–60 [PubMed: 25365976]

[14]. Cotton CC, Duits LC, Wolf WA et al. Spatial predisposition of dysplasia in Barrett's esophagus segments: a pooled analysis of the SURF and AIM dysplasia trials. Am J Gastroenterol 2015; 110: 1412–1419 [PubMed: 26346864]

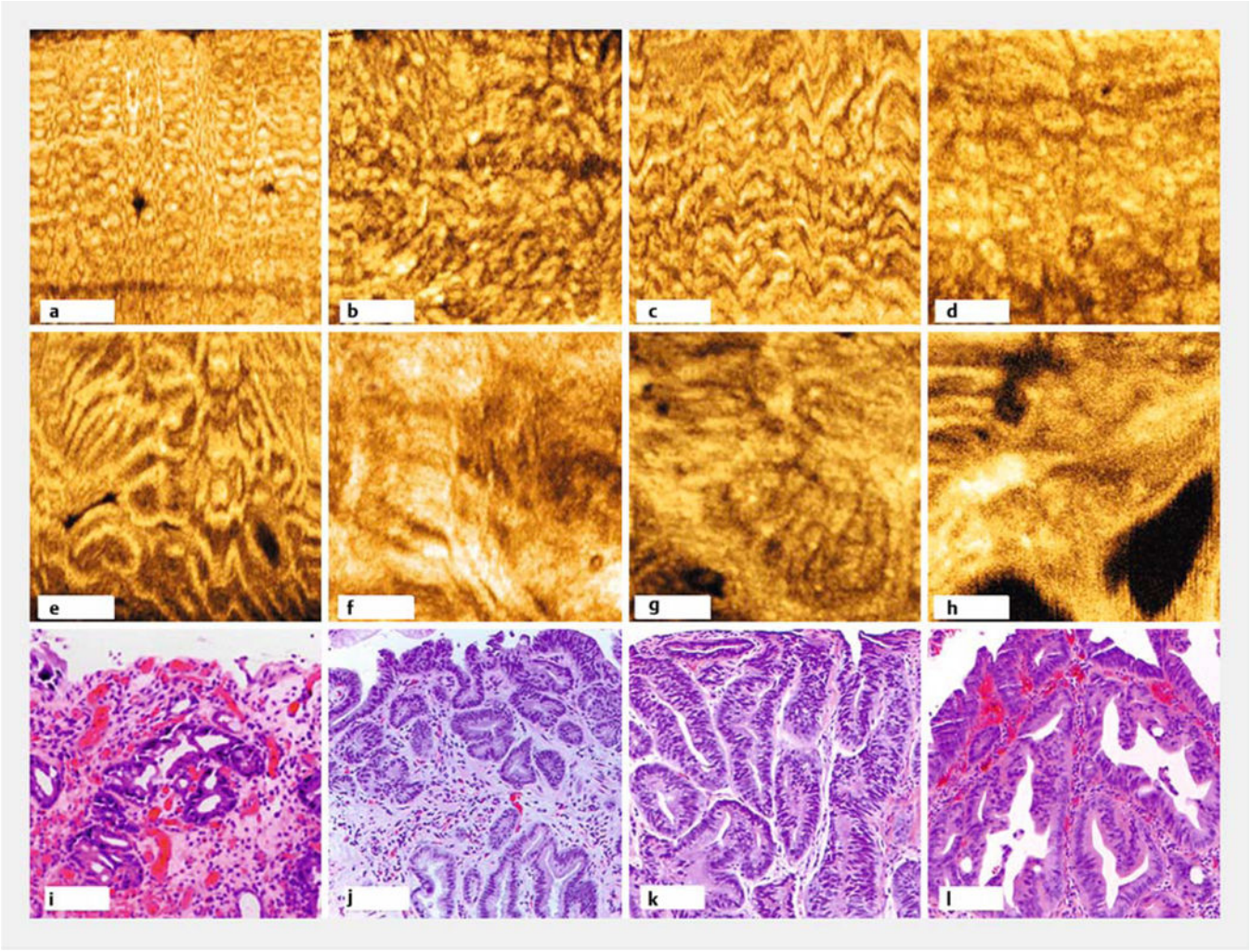

►**Fig.3.**

En face optical coherence tomography (OCT) features. **a-d** Representative regular mucosal patterns from nondysplastic Barrett's esophagus showing size and shape variations. **e-h** Irregular mucosal patterns from neoplasia showing branching, distortion, and absence of mucosal patterns. **i-l** Hematoxylin and eosin histology indicating low grade dysplasia (i), high grade dysplasia (j and k), and esophageal adenocarcinoma (l) correlated with datasets **e-h**, respectively. En face OCT cropped to highlight regions of interest. Scale bars 500 μm (**a-h**), 100μm (**i-l**).

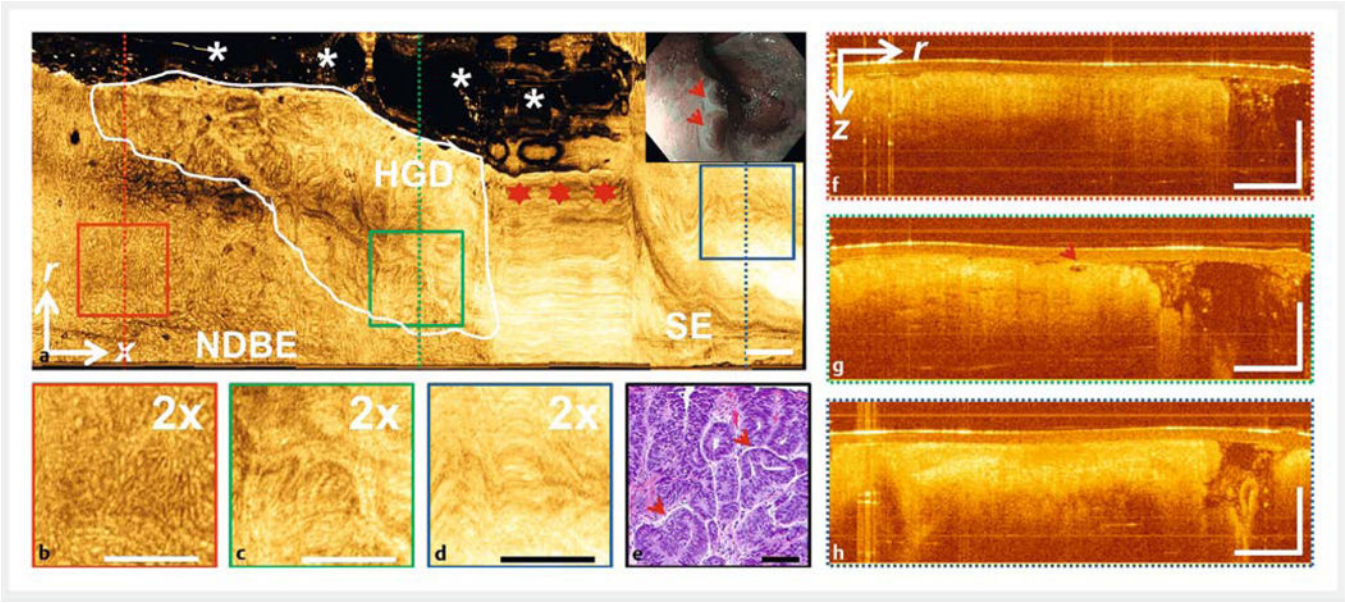

►**Fig. 5.**

Volumetric optical coherence tomography (OCT) of high grade dysplasia (HGD). **a** En face OCT at ~400pm below tissue surface. HGD region (white line) with irregular mucosal pattern adjacent to nondysplastic Barrett's esophagus (NDBE) with regular mucosal pattern and normal squamous epithelium (SE) with relatively smooth appearance and high OCT signal. Stars indicate nonuniform OCT catheter longitudinal actuation artifacts. Asterisks indicate regions where the catheter did not contact the mucosa. White-light endoscopy/ narrow-band imaging (inset) of dysplastic lesion (arrows) prior to endoscopic mucosal resection (EMR). **b-d** ×2 zoom of boxed areas in a. e Hematoxylin and eosin histology of HGD EMR specimen. **f-h** Cross-sectional OCT of dotted lines areas in a. g Atypical glandular architecture (arrow), mucosal layering present, and surface signal subsurface in the HGD region. *r*, circumferential; *x*, longitudinal; *z*, depth directions. Scale bars 100 μm (e), 1 mm (all other images).

►Table 7

Association of atypical glands co-localized under mucosal patterns, stratified according to correlated histological diagnosis and treatment history.

	Reader 1, n/N	Reader 2, n/N	Reader 3,n/N	Overall, n/N (%)	*P* value
Proportion of atypical glands under irregular mucosal patterns	21/54	23/54	27/54	71/162 (44)	<0.001[1]
■ In NDBE	10/37	10/37	13/37	33/1 11 (30)	<0.001[2]
■ Short-segment (≤ 3 cm) NDBE	8/17	7/17	7/17	22/51 (43)	0.005[3], 0.14[4]
■ Long-segment(>3cm) NDBE	2/20	3/20	6/20	11/60(18)	
■ Away (>3cm) from GEJ	1/12	1/12	3/12	5/36 (14)	0.28[4]
■ Near(≤ 3 cm) the GEJ	1/8	2/8	3/8	6/24(25)	
■ In neoplasia	11/17	13/17	14/17	38/51 (75)	
■ Treatment naïve	7/8	8/8	8/8	23/24(96)	0.001[5]
■ Previously treated	4/9	5/9	6/9	15/27 (56)	
Proportion ofatypical glands under regular mucosal patterns	13/54	10/54	10/54	33/162 (20)	
■ In NDBE	13/37	10/37	10/37	33/1 11 (30)	<0.001[6]
■ In neoplasia	0/17	0/17	0/17	0/51 (0)	

GEJ, gastroesophageal junction; NDBE, nondysplastic Barrett's esophagus.

[1] vs. proportion of atypical glands under regular mucosal patterns.

[2] vs. in neoplasia.

[3] vs. long-segment NDBE.

[4] vs. near the GEJ.

[5] vs. previously treated patients.

[6] vs. proportion of atypical glands under regular mucosal patterns in neoplasia.